Energy efficiency of power-adaptive spatial diversity methods

Olli Apilo, *Student Member, IEEE,* Mika Lasanen, Sandrine Boumard, and Aarne Mämmelä, *Senior Member, IEEE*

***Abstract*—The energy efficiency of power-adaptive multiple-input multiple-output (MIMO) diversity methods is studied in this paper. The considered diversity methods are antenna selection (AS), maximum ratio transmission (MRT), and equal gain transmission (EGT) at the transmitter and maximum ratio combining (MRC) at the receiver. The transmitter energy efficiency is evaluated using the average power amplifier (PA) efficiency and the transceiver energy efficiency is evaluated using the bit error rate (BER) as a function of average PA input signal-to-noise ratio (SNR), which is a new metric. With the new metric, the effect of the PA efficiency is taken into account in the performance evaluation. The analytical results are verified by Monte Carlo simulations. It is shown that larger diversity in the spatial or frequency domain improves the average PA efficiency in a system with channel inversion. The BER results show that the performance improvement from channel inversion diminishes due to the nonideal PA efficiency. Even though MRT is the received SNR maximizing transmitter diversity method, EGT requires less PA input energy per bit when a PA with nonideal efficiency is used. These conclusions could not have been reached using the traditional SNR metrics that do not measure the PA input energy.**

***Index Terms*—Energy efficiency, power amplifier, MIMO diversity, power control**

I. Introduction

Wireless communication systems can be divided into energy and power limited systems [1]. Because of the energy conservation law, all systems are fundamentally energy limited. However, some systems are better characterized as power limited because the electrical components have maximum operating power and transmitted power level is constrained by regulations. In wireless communications, base stations are typically considered as power limited and mobile terminals as energy limited due to the limited capacity of batteries. Wireless networks are increasingly considered as energy limited because the energy consumed by future networks is about to increase [2]. The growth in energy consumption is predicted to cause increases in the CO_2 emissions and in the operational costs of telecommunications networks. Thus, there are both environmental and economical reasons for improving the energy efficiency in cellular networks [3].

Manuscript received February 22, 2012; revised September 14, 2012 and April 23, 2013; accepted June 11, 2013. This work was done in the framework of the Celtic-Plus OPERA-Net2 project that is partly funded by Tekes – the Finnish Funding Agency for Technology and Innovation (decision number 40446/11).

O. Apilo, M. Lasanen, S. Boumard, and A. Mämmelä are with VTT Technical Research Centre of Finland, 90571 Oulu, Finland (e-mail: olli.apilo@vtt.fi; mika.lasanen@vtt.fi; sandrine.boumard@vtt.fi; aarne.mammela@vtt.fi)

Depending on the system design goals, power control can be used to achieve better error performance, higher throughput, or reduced transmission energy consumption. It is well known that the ergodic capacity of fading channels is maximized under the given average power constraint using water-filling (WF) as the power control rule [4]. The idea of WF is to allocate more power and higher data rate when the channel conditions are good. Power control is commonly used in the uplink of modern wireless communication systems such as 3G Long Term Evolution (LTE) to keep the received power from different users at the same level. These practical closed-loop power control methods are based on the idea of channel inversion [4]. Channel inversion allocates power inversely proportional to the channel gain under the given average power constraint. If the power budget allows inversion of all possible channel fades, the received power level stays constant.

We focus on studying the energy efficiency of wireless communications over a single link. We consider the system in this paper as energy limited because energy is a fundamental system resource. In addition, we also take into account the power limit set by the power amplifier (PA). We further divide the problem into transmitter and transceiver energy efficiency. Transmitter energy efficiency measures how efficiently energy from the direct current (DC) power supply is transformed into radio frequency (RF) energy while transceiver energy efficiency measures how efficiently the DC input energy is transformed into received energy and how efficiently it is used for symbol detection. Transceiver energy efficiency is suitable for comparing systems with the same bit rate while transmitter energy efficiency is suitable also for systems with variable rate. In this paper, the transmitter energy efficiency is evaluated using the average PA efficiency and the transceiver energy efficiency is evaluated using the bit error rate (BER) as a function of average PA input signal-to-noise ratio (SNR). As the PA is the main contributor to energy consumption in cellular base stations and mobile terminals [3], we restrict our focus on the efficiency of signal amplification.

For continuous transmission, transmitted power per symbol equals the transmitted energy per symbol if the symbol interval is normalized to unity. The power levels can be applied for studying energy limited systems with discontinuous transmission when expurgation is used in averaging. Expurgation means ignoring the time instants when no power is transmitted [1]. Expurgation effectively changes the power efficiency into energy efficiency. Since the link energy efficiency is studied in this paper, the expurgation is consistently used throughout this paper.

The instantaneous PA efficiency is defined as the ratio of PA output power to the PA input power. In most practical applications, the power from other inputs than DC power supply is negligible. Thus the drain efficiency, defined as the ratio of RF output power to the DC-input power [5], is widely used as an efficiency metric. The instantaneous efficiency is usually optimized for the maximum output power and the efficiency decreases when output power is decreased. In a power-adaptive system, the PA output power is a random variable and the average efficiency is a more useful metric for transmitter energy efficiency [6]. The average efficiency of a PA was defined in [7] using the probability distribution of the output power. Calculating the average PA efficiency for practical output power distributions has been considered e.g. in [8]–[10]. The distribution of the instantaneous transmitted power depends on the input signal amplitude modulation and on the power control rule. The distributions for transmitted power in some power-controlled systems were derived in [1]. These distributions were combined with the knowledge of the PA efficiency curve in [11].

The performance of diversity methods is typically measured by BER as a function of average received SNR. This metric essentially measures how well the receiver is matched to the channel but it does not consider how much energy was consumed for transmission. When we are interested in the link energy efficiency, it is also important to know how well the transmitted signal is matched to the channel, including the power amplifier. The use of BER as a function of average transmitted SNR for measuring the performance of adaptive transmission systems is emphasized in [1]. However, the average transmitted SNR does not directly measure the consumed energy because most of the PAs consume varying amount of energy depending on the transmitted RF energy. In most of the energy efficiency studies, PA efficiency is modelled as a constant. Although the effect of nonconstant PA instantaneous efficiency to the energy efficiency has been taken into account e.g. in [12]–[14], it has not been earlier considered in the BER analysis. The effect of PA nonidealities to BER has been partially taken into account in [15] where different modulation methods have been compared in the additive white Gaussian noise (AWGN) channel with respect to their peak transmitted power rather than average received SNR. This kind of comparison takes into account the limited maximum output power of PAs, which is a form of nonlinearity.

In this paper, we extend the results from [1], [11] and derive the probability density function (pdf) of the transmitted power for several power-controlled multi-antenna diversity systems. The resulting pdfs are used for calculating the average efficiency of the PA. For the transceiver energy efficiency evaluation, we introduce a new metric that can be used for comparing the amount of DC input energy needed for the target error performance level. The metric, BER as a function of average PA input SNR, is defined as the mean of the ratio of PA input energy taken from the power supply to the receiver noise spectral density. We show that the PA input SNR effectively captures the effect of power amplification efficiency when it is used in BER performance comparison.

Some of the results in this paper for the transmitted power pdfs and for the average PA efficiency in a frequency-nonselective channel have earlier been published in our conference paper [16]. The main new contributions in this paper are the introduction of BER as a function of PA input SNR as a transceiver energy efficiency metric and the energy efficient BER comparison of spatial diversity methods with and without channel inversion.

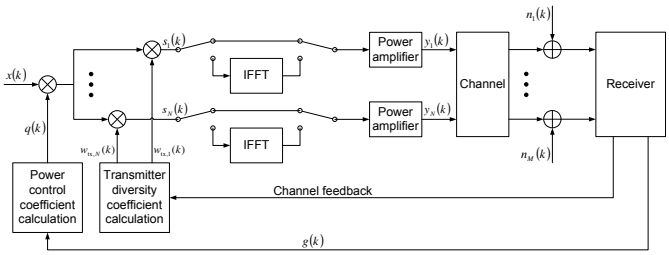

Fig. 1. Block diagram of the simplified complex baseband equivalent of the system.

The remainder of this paper is organized as follows: In Section II we present the system model and describe the used diversity methods. The analytical results for the transmitted power pdf and BER as a function of average PA input SNR are presented in Sections III and IV, respectively. The analytical results are compared to the results from Monte Carlo simulations in Section V. Finally, conclusions are drawn in Section VI.

II. System Model

The block diagram of the complex baseband equivalent of the multiple-input multiple-output (MIMO) system under study is shown in Fig. 1. The input signal $x(k)$ at time k is assumed to have constant unit amplitude. This is valid e.g. when the input signal is mapped according to phase shift keying. Both the single-carrier and orthogonal frequency division multiplexing (OFDM) transmitter are depicted by the block diagram. In case of the OFDM transmitter, the multiplication by the power control and transmitter diversity coefficients are carried out for each subcarrier independently. Inverse fast Fourier transform (IFFT) is applied before the transmitted signal amplification. The addition of the cyclic prefix has been intentionally left out from Fig. 1 for simplicity. We wanted to restrict this paper to consider two extreme cases of input signals, i.e. constant amplitude signal and OFDM signal, with respect to their amplitude distribution. When the constant amplitude signal is considered, it is easier to see the effects of power adaptation by power control and transmitter diversity. On the other hand, amplification of the OFDM signal is an important worst case due to the high peak-to-average power ratio (PAPR) from the PA efficiency point of view.

A. Channel model

In the single-carrier system, the channel is modelled according to the frequency-nonselective Rayleigh or Rician block fading model. In block fading, the channel state is constant during N_s samples and then changes to a new, independent state. The channel block duration is $N_s = 1$ for the

single-carrier system and $N_s = N_{\text{FFT}}$ for the multicarrier system, where N_{FFT} is the Fast Fourier Transform (FFT) size. At time k, the state of the channel in a system with N transmitting antennas and M receiving antennas can be given as an $M \times N$ channel matrix $\mathbf{H}(k) = [h_{m,n}(k)]_{m,n=1}^{M,N}$. Channel matrix element $h_{m,n}(k)$ then refers to the impulse response for the subchannel between antennas N and M. As Rician and Rayleigh fading are modelled as a complex-valued Gaussian process, the subchannel power gains are independent because the diversity branches between different antennas are assumed to be uncorrelated. In Rician fading, the power gain of each subchannel equals $\Gamma = |h_{m,n}(k)|^2 = \sigma^2 Y$ where σ^2 is the fading variance and Y is noncentrally chi-square distributed random variable with two degrees of freedom and noncentrality parameter $\lambda = s^2/\sigma^2$ where s is the magnitude of the line-of-sight (LOS) component. The pdf and cumulative distribution function (cdf) of Γ can be derived with the help of pdf and cdf of Y (see e.g. [17])

$$f_\Gamma(\Gamma) = \frac{1}{\sigma^2} f_Y\left(\frac{\Gamma}{\sigma^2}\right) = \frac{1}{2\sigma^2} e^{-\frac{\Gamma+s^2}{2\sigma^2}} I_0\left(\sqrt{\frac{s^2\Gamma}{\sigma^4}}\right) \tag{1}$$

and

$$F_\Gamma(\Gamma) = F_Y\left(\frac{\Gamma}{\sigma^2}\right) = 1 - Q_1\left(\frac{s}{\sigma}, \frac{\sqrt{\Gamma}}{\sigma}\right). \tag{2}$$

The average power gain is simply $E[\Gamma] = 2\sigma^2 + s^2$. Rayleigh fading is a special case of Rician fading without the LOS component, i.e. $s = 0$.

The combined channel gain is defined as the total channel power gain after all diversity processing. The upper limit for the average combined channel gain is the sum of all subchannel power gains. The fading parameters are fixed in this paper to $s^2 = 1/6$ and $\sigma^2 = 1/24$ for Rician fading and $\sigma^2 = 1/8$ for Rayleigh fading. These parameters set the upper limit for the average combined channel gain with 4 diversity branches to unity in both channel models and the K factor of Rician fading to $K = s^2/(2\sigma^2) = 2$.

In the multicarrier system, the channel is modelled as a frequency-selective tapped delay line with L distinguishable taps. Each tap $h_{m,n}(k,l)$ is modelled as flat Rayleigh fading with mean power gain of $2\sigma_l^2$. The number of taps and the mean power gain for each tap is governed by the power-delay profile. We use the classic exponential power-delay profile [18] suitable for modelling an urban environment. With exponential power-delay profile, the channel power gain as a function of delay τ can be given as

$$E\left[|h_{m,n}(k,\tau)|^2\right] = \frac{1}{\tau_d} e^{-\tau/\tau_d} \tag{3}$$

where τ_d is the root mean square (rms) delay spread of the channel. When considering a tapped delay line channel, (3) is sampled at delays $\tau = 0, 1/f_s, 2/f_s, \ldots, L/f_s$ where f_s is the sampling frequency of the system. The used power-delay profile has been normalized such that

$$E\left[\sum_{l=1}^{L} |h_{m,n}(k,l)|^2\right] = 1/4. \tag{4}$$

In an OFDM system, the channel frequency response for subcarrier $i = 0, \ldots, N_{\text{FFT}} - 1$ is given by

$$H(k,i) = \sum_{l=0}^{L-1} h(k,l) e^{-\frac{j2\pi il}{N_{\text{FFT}}}}. \tag{5}$$

Using the properties of the linear combinations of independent normal distributed random variables, it can be shown that $|H(k,i)|^2$ is centrally chi-square distributed with two degrees of freedom and mean of $2(\sigma_1^2 + \ldots + \sigma_L^2)$. Given the average normalization in (4), the pdf of $|H(k,i)|^2$ equals the pdf of Γ for the frequency-nonselective Rayleigh fading channel. Throughout the paper, it is assumed that the cyclic prefix length $N_{\text{CP}} > L$ and $N_{\text{CP}} \ll N_{\text{FFT}}$.

B. Power amplifier model

Three classes of PAs are considered in this paper: class-A, class-B, and class-G. The instantaneous drain efficiency $\eta(P)$ of class-A PA increases linearly with the increased output power P and reaches its maximum 50 % at the maximum output power P_{max} [5]. Thus, the instantaneous drain efficiency of class-A PA is simply given by

$$\eta(P) = \frac{P}{2P_{\text{max}}}, \qquad 0 < P \leq P_{\text{max}}. \tag{6}$$

The instantaneous efficiency $\eta(P)$ of class-B PA increases linearly with the output RF voltage and reaches its maximum 78.5 % at the maximum output power P_{max}. More precisely, the instantaneous drain efficiency of class-B PA is given by [19]

$$\eta(P) = \frac{\pi}{4}\sqrt{\frac{P}{P_{\text{max}}}}, \qquad 0 < P \leq P_{\text{max}}. \tag{7}$$

A class-G PA uses more than one supply voltage and at least two pairs of active devices are connected to them [20]. The switching of supply voltages is visible in the efficiency curve as a discontinuation point. The instantaneous drain efficiency for class-G PA is given by [21]

$$\eta(P) = \begin{cases} \sqrt{\frac{P\alpha}{P_{\text{max}}}}, & 0 < P \leq \frac{P_{\text{max}}}{\alpha} \\ \sqrt{\frac{P}{P_{\text{max}}}}, & \frac{P_{\text{max}}}{\alpha} < P < P_{\text{max}} \end{cases} \tag{8}$$

where $\alpha > 1$ is the factor defining the switching point at the output power range. In this paper, we have consistently used the value $\alpha = 2$ that sets the switching point in the middle of the output power range. The other characteristics than the instantaneous efficiency as well as the design of the PA classes considered here can be found from [19]

The average PA efficiency is used as the transmitter energy efficiency metric in this paper. It is useful for comparing different PA designs, when the transmission and reception methods are fixed. Traditionally the efficiency of PAs is defined as the power ratio and the average PA efficiency is defined as the ratio of the mean output power to the mean input power [7]. As discussed in Section I, power efficiency can be transformed into energy efficiency by using expurgation in averaging. Combining the definition of average PA efficiency

from [22] to the concept of expurgation, the average PA efficiency $\overline{\eta}$ can be calculated as

$$\overline{\eta} = \frac{1}{1-\mathbb{P}_{\text{out}}} \int_0^{P_{\max}} \eta(P) f_P(P) \mathrm{d}P \tag{9}$$

where $\mathbb{P}_{\text{out}}$ is the probability of outage, $1/(1-\mathbb{P}_{\text{out}})$ is the expurgation term, and $f_P(P)$ is the transmitted power pdf.

Closed-form expressions for $f_P(P)$ in OFDM systems exist only in certain special cases, see Section III-B. However, there is a method to calculate the average PA efficiency when the channel is frequency-nonselective [11]. The instantaneous efficiency $\eta(P)$ in (9) is replaced by $\eta_{\text{OFDM}}(P)$

$$\begin{aligned}\eta_{\text{OFDM}}(P) = &\int_0^{\frac{P_{\max}}{P}} \eta(PX) f_X(X) \mathrm{d}X \\ &+ \eta(P_{\max}) \int_{\frac{P_{\max}}{P}}^{\infty} f_X(X) \mathrm{d}X\end{aligned} \tag{10}$$

where $f_X(X)$ is the pdf of the OFDM signal power and pdfs [11, Eqs. (11)-(14)], (23), and (24) are used as $f_P(P)$.

PAs are assumed to be linear until their maximum output power at which the input signal amplitudes greater than $P_{\max}$ are clipped due to saturation. This soft limiting model sets a practical power constraint to the energy limited system. The power at the output of the nth PA is then for the single-carrier system

$$P_n(k) = \min(P_{\max}, \overline{P}|s_n(k)|^2) \tag{11}$$

where $\overline{P}$ is the gain from signal amplification and $s_n(k)$ is the transmitted signal after power control and transmitter diversity processing, see Fig. 1. We have normalized the power control and transmitter diversity coefficients such that $\overline{P}$ also equals total average transmitted power from all antennas. In the OFDM system, the IFFT operation is applied before the signal amplification and the power at the PA output for the OFDM system is

$$P_n(k) = \min\left(P_{\max}, \frac{\overline{P}}{\sqrt{N_{\text{FFT}}}} \left| \sum_{i=0}^{N_{\text{FFT-1}}} s_n(k) e^{-\frac{j2\pi ik}{N_{\text{FFT}}}} \right|^2 \right). \tag{12}$$

It is also assumed that the PA input power during outage is zero.

The average PA efficiency for OFDM systems is degraded by the high PAPR. The theoretical upper bound of PAPR for an OFDM system with phase modulated symbols is N_{FFT} [23]. In order to avoid the nonlinear clipping effects from the soft limiting PA, the average output power level $\overline{P}$ has to be set low enough. More precisely, the output power backoff $10\log_{10}(P_{\max}/\overline{P})$ has to be set so high that $\mathbb{P}(P_n(k) = P_{\max}) \approx 0$. The effect of high PAPR on the average PA efficiency is illustrated in Section V-B.

C. Power control

We consider three fundamental power control rules that have a perfect knowledge of the combined channel gain $g(k)$ [4]. In addition to the average power constraint set in [4], we additionally set a constraint to the maximum output power that corresponds to the saturation level of the soft-limiting PA. The corresponding power constraint equation is

$$\begin{aligned}&\int_0^{\infty} \min\left(P_{\max}, P(g)\right) f_g(g) \mathrm{d}g \\ &= \int_0^{\infty} \min\left(P_{\max}, \overline{P}|q(g)|^2\right) f_g(g) \mathrm{d}g = \overline{P}\end{aligned} \tag{13}$$

where q is the power control coefficient. The WF solution maximizes the throughput subject to the power constraints. The WF power control coefficient can be given as

$$q(k) = \begin{cases} \sqrt{1/\mu_{\text{wf}} - 1/g(k)}, & g(k) \geq \mu_{\text{wf}} \\ 0, & \text{otherwise} \end{cases} \tag{14}$$

where μ_{wf} is the cut-off value solved from (13). In this study, adaptive modulation is not used with WF, i.e. rate adaptation is done by changing the code rate or the symbol interval. If an additional constraint is set such that the received power is constant $P_{\text{rx}} = \overline{P}\beta$, the throughput is maximized by truncated channel inversion (TCI). The power control coefficient for TCI is given by

$$q(k) = \begin{cases} \sqrt{\beta/g(k)}, & g(k) \geq \mu_{\text{ci}} \\ 0, & \text{otherwise} \end{cases} \tag{15}$$

where β is a constant solved from (13) and μ_{ci} is the the cut-off value calculated from the selected outage probability $\mathbb{P}_{\text{out}} = \mathbb{P}(g < \mu_{\text{ci}})$. For full channel inversion (FCI), no outages are allowed and thus $\mu_{\text{ci}} = 0$. We are using the same definition of the outage probability as in [4]. Another common way is to define the outage probability using the mutual information and the target rate, see e.g. [24]. However as noted in [24], the mutual information is a function of channel gain and thus the two definitions are related. In the OFDM system, transmission power is constrained in the long term sense, i.e. the average power of a single OFDM symbol is not constrained. With this assumption, power control can be done for each subcarrier individually using subcarrier-wise combined channel gain $g(k,i)$.

D. Diversity methods

Maximum ratio combining (MRC) [25] is selected as the single-input multiple-output (SIMO) receiver diversity method in this paper. MRC coherently weights and sums the signals from different diversity branches such that combined channel gain $g_{\text{mrc}}(k)$ is the sum of subchannel power gains $g_{\text{mrc}}(k) = \sum_{m=1}^{M} |h_{m,1}(k)|^2 = \sum_{m=1}^{M} \sigma^2 Y = \sigma^2 \sum_{m=1}^{M} Y$. The sum of independent noncentrally chi-square distributed random variables with the common noncentrality parameter $\lambda = s^2/\sigma^2$ is noncentrally chi-square distributed with the noncentrality parameter $M\lambda$ [17]. Thus, the pdf and cdf of g_{mrc} in Rician fading are given by

$$f_{g_{\text{mrc}}}(g) = \frac{1}{2\sigma^2} \left(\frac{g}{Ms^2}\right)^{\frac{M-1}{2}} e^{-\frac{g+Ms^2}{2\sigma^2}} \cdot I_{M-1}\left(\sqrt{\frac{Ms^2 g}{\sigma^4}}\right) \tag{16}$$

and

$$F_{g_{\text{mrc}}}(g) = 1 - Q_M\left(\frac{\sqrt{M}s}{\sigma}, \frac{\sqrt{g}}{\sigma}\right). \tag{17}$$

Distributions (16) and (17) can be applied to Rayleigh fading by setting $s = 0$.

The simplest closed-loop transmitter diversity technique is to select the antenna that results in the highest total received power and use only this antenna for transmission. This method is commonly called antenna selection (AS). When there are multiple antennas also at the receiver, it is possible to combine transmitter AS to MRC [26]. Then the combined channel gain becomes $g_{\text{as/mrc}}(k) = \max(\sum_{m=1}^{M} |h_{m,1}(k)|^2, \ldots, \sum_{m=1}^{M} |h_{m,N}(k)|^2)$. Using (16) and (17), the pdf of $g_{\text{as/mrc}}(k)$ can be written as

$$f_{g_{\text{as/mrc}}}(g) = N F_{g_{\text{mrc}}}^{N-1}(g) f_{g_{\text{mrc}}}(g). \tag{18}$$

The maximum ratio transmission (MRT) combined with MRC (MRT/MRC) is the optimal transmitter diversity technique in the sense that it maximizes the received SNR [27]. The optimal $N \times 1$ transmission and $M \times 1$ reception weight vectors $\mathbf{w}_{\text{tx}}$ and $\mathbf{w}_{\text{rx}}$ can be presented compactly with the help of singular value decomposition (SVD) of the channel matrix [28]. Given SVD $\mathbf{H} = \mathbf{U}\mathbf{D}\mathbf{V}^H$, the optimal weight vectors are $\mathbf{w}_{\text{tx}} = \mathbf{v}_{\max}$ and $\mathbf{w}_{\text{rx}} = \mathbf{u}_{\max}^H$ where $\mathbf{v}_{\max}$ and $\mathbf{u}_{\max}$ are the principal singular vectors of $\mathbf{H}$, i.e. the column vectors of $\mathbf{U}$ and $\mathbf{V}$ corresponding to the maximum singular value $d_{\max}$. The resulting combined channel gain can be shown to be $g_{\text{mrt/mrc}}(k) = d_{\max}^2$ [28]. The pdf of $g_{\text{mrt/mrc}}(k)$ is presented in [29]. In the special multiple-input single-output (MISO) case, it is possible to present $\mathbf{w}_{\text{tx}}(k)$ as a simple function of subchannel power gains [30]

$$w_{\text{tx},n}(k) = \frac{h_{1,n}^*(k)}{\sqrt{\sum_{i=1}^{N} |h_{1,i}(k)|^2}}. \tag{19}$$

Even though MRT/MRC is optimal in terms of the received SNR, it is not favoured in practical systems because of its variable transmitted power per antenna. A transmitter diversity method that keeps the transmitted power constant and only adapts the phase of the transmitted signal is called equal gain transmission (EGT) [31]. The optimal EGT/MRC transmitter and receiver weights fulfill [32]

$$(\mathbf{w}_{\text{tx}}, \mathbf{w}_{\text{rx}}) = \arg \max_{\mathbf{w}_{\text{tx}}, \mathbf{w}_{\text{rx}}} \left| \mathbf{w}_{\text{rx}}^H \mathbf{H} \mathbf{w}_{\text{tx}} \right| \tag{20}$$

where $w_{\text{tx},n} = \exp(j\theta_n)/\sqrt{N}$ and $\mathbf{w}_{\text{rx}} = \mathbf{H}\mathbf{w}_{\text{tx}}/||\mathbf{H}\mathbf{w}_{\text{tx}}||_2$. No unique closed-form solution exists for (20). An EGT solution almost reaching the received SNR of MRT/MRC has been given in [32]

$$\mathbf{w}_{\text{tx}} = \frac{1}{\sqrt{N}} \left(1 \; e^{j(\theta_2 - \theta_1)} \; e^{j(\theta_3 - \theta_1)} \; \cdots \; e^{j(\theta_N - \theta_1)} \right)^T \tag{21}$$

where $(\theta_1 \; \theta_2 \cdots \theta_N)$ are the phases of the principal right singular vector of the channel matrix. The pdf of the combined channel gain or received SNR has not been presented in the literature.

III. Probability distribution function of the transmitted power

As can be seen from (9), (38), and (39), the pdf of the transmitted power is needed for calculating the average PA efficiency and the average PA input SNR. We start presenting the analytical results for the transmitted power pdf for the constant amplitude input signal $x(k)$ first in a single-carrier system and then in an OFDM system.

A. Single-carrier system

The transmitted power pdfs for WF and TCI were presented in [11, Eqs. (11)-(14)] for a single-input single-output (SISO) system. The same results can be applied to MRC and AS/MRC by using the pdfs of the combined channel gain from (16) and (18), respectively.

MRT/MRC can be considered as a special case of power control in which the average transmitted power $\overline{P}$ is divided among the transmitting antennas. The maximum transmitted power from a single antenna is constrained to $\overline{P}$ because no additional power control is used, i.e. $q(k) = 1$, and according to the properties of SVD, $0 < |w_{\text{tx},n}(k)| < 1$. Now if we set $\overline{P} = P_{\max}$, the signal is never saturated at the PA and the transmitted power is simply $P_n(k) = \overline{P}|s_n(k)|^2 = \overline{P}|w_{\text{tx},n}(k)|^2$.

Let us first consider the special case of MISO MRT. The transmitted power is

$$\begin{aligned} P_n(k) &= \overline{P} \frac{|h_{1,n}(k)|^2}{\sum_{i=1}^{N} |h_{1,i}(k)|^2} \\ &= \overline{P} \frac{|h_{1,n}(k)|^2}{|h_{1,n}(k)|^2 + \sum_{i \neq n} |h_{1,i}(k)|^2} \\ &= \overline{P} \frac{\sigma^2 Y_1}{\sigma^2 Y_1 + \sigma^2 Y_2} = \overline{P} \frac{Y_1}{Y_1 + Y_2} \end{aligned} \tag{22}$$

where Y_1 is noncentrally chi-square distributed with $n_1 = 2$ degrees of freedom and noncentrality parameter $\lambda_1 = s^2/\sigma^2$. Y_2 is noncentrally chi-square distributed with $n_2 = 2(N-1)$ degrees of freedom and noncentrality parameter $\lambda_2 = (N-1)s^2/\sigma^2$. Using Theorem 1 from [33], the transmitted power pdf of MISO MRT in Rician fading can be given as

$$\begin{aligned} f_{P_n}(P) = {} & \frac{1}{\overline{P}} e^{\left(-\frac{Ns^2}{2\sigma^2}\right)} \\ & \times \sum_{i=0}^{\infty} {}_2F_1 \left(-i, -i; N-1; \frac{(N-1)(1 - P/\overline{P})}{P/\overline{P}} \right) \\ & \times \frac{\left(s^2/(2\sigma^2)\right)^i}{i!} \frac{(P/\overline{P})^i (1 - P/\overline{P})^{N-2}}{B(i+1, N-1)}, \quad 0 < P < \overline{P} \end{aligned} \tag{23}$$

where ${}_2F_1(a, b; c; z)$ is the ordinary hypergeometric function and $B(x, y)$ is the beta function. Again, the transmitted power pdf for Rayleigh fading can be achieved by inserting $s = 0$ to (23). The resulting pdf has a simple form

$$f_P(P) = \frac{N-1}{\overline{P}} \left(1 - \frac{P}{\overline{P}} \right)^{N-2}, \quad 0 < P < \overline{P}. \tag{24}$$

The problem of finding the transmitted power distribution from a single antenna in the general MIMO MRT/MRC case is equivalent of finding the distribution of the squared amplitude of the elements of the principal singular vector $\mathbf{v}_{\max}$. There are no readily applicable results to this problem to the knowledge of the authors. Our intuition says that the distribution in the MIMO case should be close to that in the MISO case. In

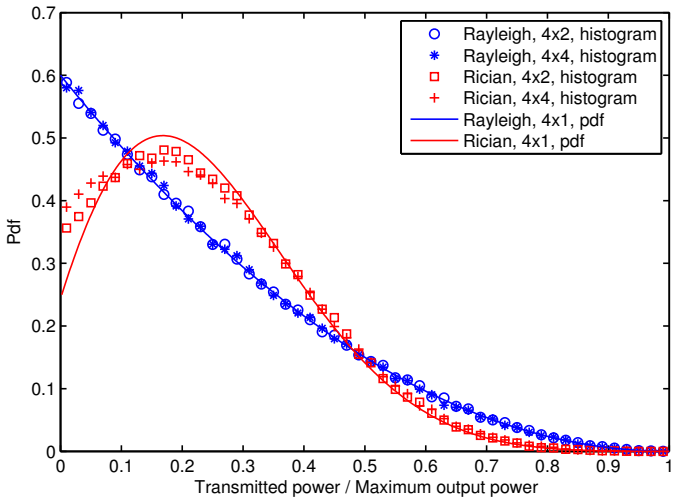

Fig. 2. Pdfs of MISO MRT in a single carrier system compared to sample histograms of MIMO MRT/MRC with average total transmitted power from all antennas $\overline{P} = P_{\max}$.

order to confirm this, the Kolmogorov-Smirnov test [34] was applied to the transmitted power samples generated using the channel parameters from Section II. According to the test in Rayleigh fading, the transmitted power distribution was the same in 2×1, 2×2, and 2×4 cases as well as 4×1, 4×2, and 4×4 cases with the significance level of 5%. For Rician fading, the distributions in the MISO and MIMO cases were not the same. To illustrate the test results, pdfs (23) and (24) are shown together with sample histograms in Fig. 2. It can be seen that in Rician fading the MISO pdf matches well to the MIMO histograms at high power levels.

B. OFDM system

Power control and transmitter diversity in an OFDM system are done subcarrierwise before the IFFT operation based on the channel frequency response. In typical channel conditions, the channel frequency response is correlated over subcarriers. The level of correlation is determined by the channel coherence bandwidth that is inversely proportional to the channel delay spread τ_d. The output signal power from IFFT can be then given as the sum of dependent random variables. Generally, the calculation of the sum of dependent random variables requires the knowledge of the joint pdf of all added random variables. The number of dependent random variables can be several thousands in wideband OFDM systems making the accurate analysis mathematically intractable. On the other hand for a channel with exponential power delay profile, there is a strong dependence between subcarriers prohibiting the use of central limit theorems for functions of independent or weakly dependent random variables [35]. To get a better understanding on the transmitted power distribution in typical channel conditions, we consider two extreme cases: the flat fading channel and the highly frequency-selective channel with independent channel frequency responses on adjacent subcarriers.

When the channel is frequency-nonselective, each frequency domain symbol is multiplied with the same power control and transmitter diversity coefficient. Because of the linearity of the IFFT operation, the transmitted power pdf is the same whether transmitted signal weighting is done in frequency or time domain, i.e. before or after IFFT. For the latter case, the transmitted power can be given as $P_n(k) = \min(P_{\max}, \overline{P}XQ)$ where

$$X = \frac{1}{\sqrt{N_{\text{FFT}}}} \left| \sum_{i=0}^{N_{\text{FFT-1}}} x(k) e^{-\frac{j2\pi ik}{N_{\text{FFT}}}} \right|^2 \tag{25}$$

and $Q = |q(k)w_{\text{tx},n}(k)|^2$ are independent random variables representing the power of the OFDM signal and the squared amplitude of transmitter weight coefficients, respectively. According to the central limit theorem, the power of an OFDM signal sample is approximately exponentially distributed with pdf $f_X(X) = e^{-X}$.

In our analysis, an explicit solution for the transmitted power pdf in a SIMO OFDM system with TCI, MRC, and flat Rayleigh fading channel was found. Using Eq. (5-5) from [36] to (15), the pdf of Q can be given as

$$\begin{aligned} f_Q(Q) &= \frac{\beta}{Q^2} f_g\left(\frac{\beta}{Q}\right) \\ &= \frac{\beta}{2\sigma^2 Q^2 (M-1)!} \left(\frac{\beta}{2\sigma^2 Q}\right)^{M-1} e^{-\frac{\beta}{2\sigma^2 Q}}. \end{aligned} \tag{26}$$

Given pdfs for X and Q, the pdf of $W = XQ$ can be calculated using the theorem for the product of two random variables [37]

$$\begin{aligned} f_W(W) &= \int_0^{\beta/\mu_{\text{ci}}} \frac{1}{Q} f_Q(Q) f_X\left(\frac{W}{Q}\right) \mathrm{d}Q \\ &= \left(\frac{\beta}{2\sigma^2}\right)^M \frac{1}{(M-1)!} \int_0^{\beta/\mu_{\text{ci}}} \frac{1}{Q^{M+2}} e^{-\frac{\beta+2\sigma^2 W}{2\sigma^2 Q}} \mathrm{d}Q. \end{aligned} \tag{27}$$

The expression in (27) can be modified to the familiar form of upper incomplete Gamma function by the change of variables $z = -(\beta + 2\sigma^2 W)/(2\sigma^2 Q)$ and the outcome after some manipulation is

$$\begin{aligned} f_W(W) = &\left(\frac{\beta}{2\sigma^2}\right)^M \frac{1}{(M-1)!} \left(\frac{2\sigma^2}{\beta + 2\sigma^2 W}\right)^{M+1} \\ &\times \int_{\mu_{\text{ci}}/(2\sigma^2) + \mu_{\text{ci}} W/\beta}^{\infty} z^M e^{-z} \mathrm{d}z. \end{aligned} \tag{28}$$

Now the integral in (28) is just the upper incomplete Gamma function. Since M is positive integer, (28) can be further simplified using Eq. (8.4.8) from [38]

$$\begin{aligned} f_W(W) = &\frac{2\sigma^2 M \beta^M}{(\beta + 2\sigma^2 W)^{M+1}} \\ &\times \sum_{k=0}^{M} \frac{1}{k!} \left(\frac{\mu_{\text{ci}}}{2\sigma^2} + \frac{\mu_{\text{ci}} W}{\beta}\right)^k e^{-\frac{\mu_{\text{ci}}}{2\sigma^2} - \frac{\mu_{\text{ci}} W}{\beta}}. \end{aligned} \tag{29}$$

Finally taking into account the outage and the possibility of soft limiting at the PA, the transmitted power pdf can be given as

$$f_P(P) = \begin{cases} \int_{P_{\max}}^{\infty} \frac{1}{\overline{P}} f_W\left(\frac{y}{\overline{P}}\right) \mathrm{d}y & P = P_{\max} \\ \frac{1}{\overline{P}} f_W\left(\frac{P}{\overline{P}}\right) & 0 < P < P_{\max} \\ F_g(\mu_{\text{ci}}) & P = 0 \end{cases}. \tag{30}$$

When the channel is highly frequency-selective, the channel frequency responses of all subcarriers are independent. This is equivalent to the block fading model in the frequency domain. Thus also the power control and transmitter diversity coefficients are independent for each subcarrier and according to the central limit theorem both real and imaginary parts of the IFFT output are normally distributed with zero mean and $1/(2\hat{N})$ variance where $\hat{N}$ is the number of antennas actually transmitting the signal. The transmitted power pdf is then

$$f_P(P) = \begin{cases} \int_{P_{\max}}^{\infty} \frac{\hat{N}}{\overline{P}} e^{-\frac{\hat{N}y}{\overline{P}}} \mathrm{d}y, & P = P_{\max} \\ \frac{\hat{N}}{\overline{P}} e^{-\frac{\hat{N}P}{\overline{P}}}, & 0 \le P < P_{\max} \end{cases}. \tag{31}$$

IV. BER AS A FUNCTION OF AVERAGE PA INPUT SNR

The average PA efficiency is a useful metric for evaluating the energy efficiency of the transmitter. However, it provides no information how well the transmitted signal is matched to the channel. In order to analyze how much energy is consumed in signal amplification for the target error performance level, we have defined a new metric for transceiver energy efficiency: BER as a function of average PA input SNR. BER in the single-carrier system can be calculated as

$$\overline{\mathbb{P}}_b = \frac{1}{1-\mathbb{P}_{\text{out}}} \int_0^{\infty} \mathbb{P}_b(\gamma) f_\gamma(\gamma) \mathrm{d}\gamma \tag{32}$$

where $\mathbb{P}_b(\gamma)$ is the bit error probability for the given combination of modulation and channel coding and γ is the received SNR per symbol. The expurgation term $1/(1-\mathbb{P}_{\text{out}})$ is included into the BER definition because it is meaningless to consider bit error probability when there is no transmission.

The received SNR per symbol in the single-carrier system can be given as ratio of the received signal power to the noise power at the sampling instants $\gamma = Pg/(N_0 R)$ where g is the combined channel gain, N_0 is the receiver AWGN power spectral density, and R is the symbol rate. When there is no power control, the received SNR simplifies to $\gamma = g/(N_0 R)$ because we have assumed $|x(k)|^2 = 1$, and the pdf of the received SNR is then simply $f_\gamma(\gamma) = (N_0 R) f_g(N_0 R \gamma)$. When TCI is used, the pdf of the received SNR can be shown to be

$$f_\gamma(\gamma) = \begin{cases} 1 - F_g\left(\frac{\overline{P}\beta}{P_{\max}}\right), & \gamma = \frac{\overline{P}\beta}{N_0 R} \\ \frac{N_0 R}{P_{\max}} f_g\left(\frac{N_0 R \gamma}{P_{\max}}\right), & \frac{\mu_{\text{ci}} P_{\max}}{N_0 R} \le \gamma < \frac{\overline{P}\beta}{N_0 R} \text{ and } \mu_{\text{ci}} \le \frac{\overline{P}\beta}{P_{\max}} \\ F_g(\mu_{\text{ci}}), & \gamma = 0 \end{cases}. \tag{33}$$

WF is typically used together with bit rate control. We restrict the performance analysis to diversity methods with constant bit rate. Thus, we will not consider the BER of WF here.

The PA input SNR per symbol is defined as the ratio of PA input energy from the power supply to the receiver noise spectral density. The average PA input SNR per symbol is then $\overline{\gamma}_{\text{PA}} = \overline{P}_{\text{sup}}/((1-\mathbb{P}_{\text{out}}) N_0 R)$ where we have introduced the expurgation term $1/(1-\mathbb{P}_{\text{out}})$ to convert the power ratio to the energy ratio. According to the definition of PA instantaneous efficiency, the PA input power can be given as $P_{\text{sup}} = P/\eta(P)$. It can be seen from (6) that the PA input power for class A PA is constant $P_{\text{sup}} = 2P_{\max}$. Using (7) and (8), we have

$$P_{\text{sup}} = \frac{4}{\pi}\sqrt{P P_{\max}}, \quad 0 < P_{\text{sup}} \le \frac{4}{\pi} P_{\max} \tag{34}$$

for class B PA and

$$P_{\text{sup}} = \begin{cases} \sqrt{\frac{P P_{\max}}{2}}, & 0 < P_{\text{sup}} \le \frac{P_{\max}}{2} \\ 0, & \frac{P_{\max}}{2} < P_{\text{sup}} \le \frac{P_{\max}}{\sqrt{2}} \\ \sqrt{P P_{\max}}, & \frac{P_{\max}}{\sqrt{2}} < P_{\text{sup}} \le P_{\max} \end{cases} \tag{35}$$

for class G PA.

The pdfs for PA input power can be derived using the theorem for finding the pdf of monotonous and differentiable function of a random variable [36]. The input power pdf for TCI with class B PA can be shown to be

$$f_{P_{\text{sup}}}(P_{\text{sup}}) = \begin{cases} F_g\left(\frac{\overline{P}\beta}{P_{\max}}\right) - F_g(\mu_{\text{ci}}), & P_{\text{sup}} = \frac{4}{\pi} P_{\max} \text{ and } \mu_{\text{ci}} \le \frac{\overline{P}\beta}{P_{\max}} \\ \frac{32 P_{\max} \overline{P}\beta}{\pi^2 P_{\text{sup}}^3} f_g\left(\frac{16 P_{\max} \overline{P}\beta}{\pi^2 P_{\text{sup}}^2}\right), & 0 < P_{\text{sup}} < P_{\text{lim}} \\ F_g(\mu_{\text{ci}}), & P_{\text{sup}} = 0 \end{cases} \tag{36}$$

where $P_{\text{lim}} = 4/\pi P_{\max}$ when $\mu_{\text{ci}} \le \overline{P}\beta/P_{\max}$ and $P_{\text{lim}} = \sqrt{16\overline{P}\beta P_{\max}/(\pi^2 \mu_{\text{ci}})}$ when $\mu_{\text{ci}} > \overline{P}\beta/P_{\max}$. Similarly, the input power pdfs for TCI with class G PA are

$$f_{P_{\text{sup}}}(P_{\text{sup}}) = \begin{cases} F_g\left(\frac{\overline{P}\beta}{P_{\max}}\right) - F_g(\mu_{\text{ci}}), & P_{\text{sup}} = P_{\max} \text{ and } \mu_{\text{ci}} \le \frac{\overline{P}\beta}{P_{\max}} \\ \frac{2 P_{\max} \overline{P}\beta}{P_{\text{sup}}^3} f_g\left(\frac{P_{\max} \overline{P}\beta}{P_{\text{sup}}^2}\right), & \frac{P_{\max}}{\sqrt{2}} \le P_{\text{sup}} < P_{\text{L2}} \text{ and } \mu_{\text{ci}} \le \frac{2\overline{P}\beta}{P_{\max}} \\ \frac{P_{\max} \overline{P}\beta}{P_{\text{sup}}^3} f_g\left(\frac{P_{\max} \overline{P}\beta}{2 P_{\text{sup}}^2}\right), & 0 < P_{\text{sup}} \le P_{\text{L1}} \\ F_g(\mu_{\text{ci}}), & P_{\text{sup}} = 0 \end{cases} \tag{37}$$

where $P_{\text{L1}} = P_{\max}/2$ when $\mu_{\text{ci}} \le 2\overline{P}\beta/P_{\max}$ and $P_{\text{L1}} = \sqrt{\overline{P}\beta P_{\max}/(2\mu_{\text{ci}})}$ when $\mu_{\text{ci}} > 2\overline{P}\beta/P_{\max}$. The upper limit is $P_{\text{L2}} = P_{\max}$ when $\mu_{\text{ci}} \le \overline{P}\beta/P_{\max}$ and $P_{\text{L2}} = \sqrt{\overline{P}\beta P_{\max}/\mu_{\text{ci}}}$ when $\mu_{\text{ci}} > \overline{P}\beta/P_{\max}$. With the help of transmitted power pdfs (23) and (24), the input power pdfs for MRT with class B and G PAs can be given as

$$f_{P_{\text{sup}}}(P_{\text{sup}}) = \frac{\pi^2 P_{\text{sup}}}{8 P_{\max}} f_P\left(\frac{\pi^2 P_{\text{sup}}^2}{16 P_{\max}}\right), \quad 0 < P_{\text{sup}} < \frac{4}{\pi} P_{\max} \tag{38}$$

and

$$f_{P_{\text{sup}}}(P_{\text{sup}}) = \begin{cases} \frac{2 P_{\text{sup}}}{P_{\max}} f_P\left(\frac{P_{\text{sup}}^2}{P_{\max}}\right), & \frac{P_{\max}}{\sqrt{2}} \le P_{\text{sup}} < P_{\max} \\ \frac{4 P_{\text{sup}}}{P_{\max}} f_P\left(\frac{2 P_{\text{sup}}^2}{P_{\max}}\right), & 0 < P_{\text{sup}} \le \frac{P_{\max}}{2} \end{cases}, \tag{39}$$

respectively.

The average PA input power can then be calculated using the above pdfs

$$\overline{P}_{\text{sup}} = P_{\text{sup,max}} \cdot \mathbb{P}(P = P_{\max}) + \int_0^{P_{\text{sup,max}}} P_{\text{sup}} f_{P_{\text{sup}}}(P_{\text{sup}}) \mathrm{d}P_{\text{sup}} \tag{40}$$

where $P_{\text{sup,max}} = (4/\pi)P_{\max}$ for class B PA and $P_{\text{sup,max}} = P_{\max}$ for class G PA. All the results in this section are presented for the single-carrier system. The results can be extended to the OFDM system using the transmitted power pdf from (30) when the channel is frequency-nonselective and large enough output power backoff is used to almost always avoid saturation at PA. Then there are no nonlinearities in the system and the system model is equivalent to the discrete frequency domain OFDM model presented e.g. in [39, pp. 749-752].

V. Numerical results

In this section, we verify the expressions for the average PA efficiency and for the BER as a function of PA input SNR by Monte Carlo simulations. In each result figure, the solid line represents analytically calculated values and markers represent the values from simulations. For each marker, averaging over 100000 samples was used.

A. Effect of diversity gain to the average PA efficiency

The effect of diversity gain to the average PA efficiency of class B and G PAs in the single-carrier system is illustrated in Fig. 3 where WF and TCI are selected as power control methods, MRC is used at the receiver, and the channel is modelled as the frequency-nonselective Rician fading. The outage probability for TCI is set to 10 %. The highest average PA efficiency is achieved with SISO WF for both PAs. It can be seen that increased diversity gain reduces the average efficiency of class B PA for WF. This can be explained by the instantaneous efficiency from (7) and by the shape of the transmitted power pdf. As the instantaneous efficiency increases with the output power, the best average efficiency is achieved when the probability of close-to-maximum transmitted power is high. The transmitted power pdf under the same setting as in Fig. 3 is shown in Fig. 4 and 5 with $\overline{P}/P_{\max} = 0.35$ and $\overline{P}/P_{\max} = 0.65$, respectively. Increased diversity clearly shifts the peak of the WF transmitted power pdf towards smaller transmission power decreasing the average PA efficiency. This can be explained by examining the pdf of g and P as a function of g shown in Fig. 6. The increased diversity clearly widens the pdf of g and shifts its peak closer to its average value. As shown in Fig. 6, the maximum transmitted power of WF decreases as M increases. This causes that the probability mass and the peak of the transmitted power pdf are shifted closer to the mean value $\overline{P} = 0.35P_{\max}$. Also for TCI the maximum transmitted power level decreases as M increases. However as can be seen from Fig. 6, the increased diversity also increases the minimum transmitted power level of TCI. The decrease in the extreme values of the transmitted power makes the pdf narrower and shifts the peak of the pdf closer to the mean value. At high average transmitted power in Fig. 5, the impulses at zero and at the maximum output power dominate the pdf of SISO WF. Thus, the transmission strategy is close to on-off, i.e. transmit with the maximum power or do not transmit at all. For TCI, there is no clear effect visible. However as can be seen from Fig. 4, the increased diversity gain slightly shifts the peak of the transmitted power

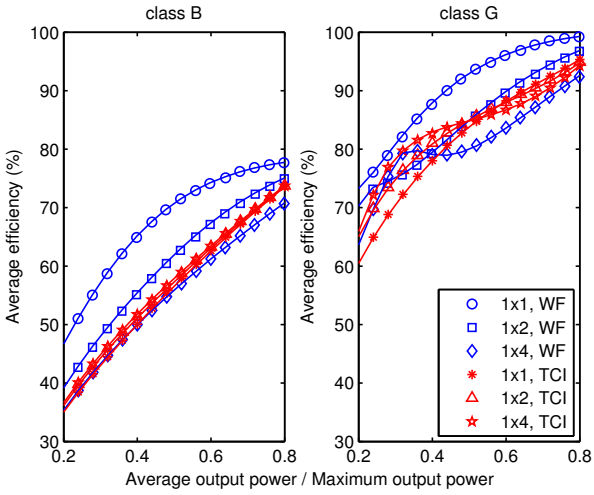

Fig. 3. Average PA efficiency in a single carrier system as a function of $\overline{P}/P_{\max}$ for power-controlled MRC in Rician fading.

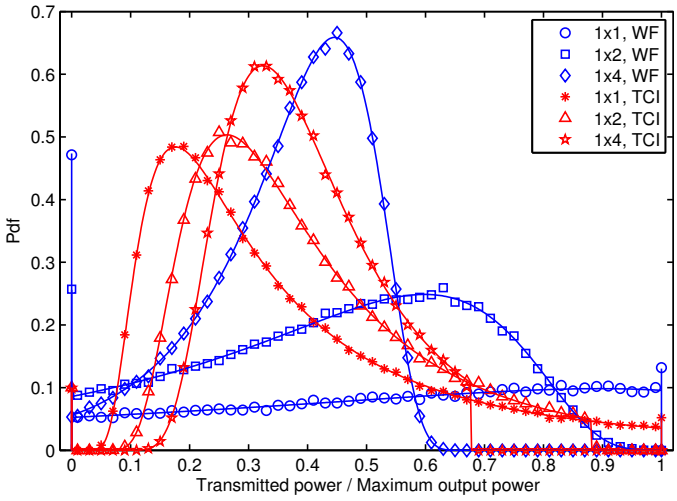

Fig. 4. Transmitted power pdf in a single carrier system for power-controlled MRC and $\overline{P}/P_{\max} = 0.35$ in Rician fading.

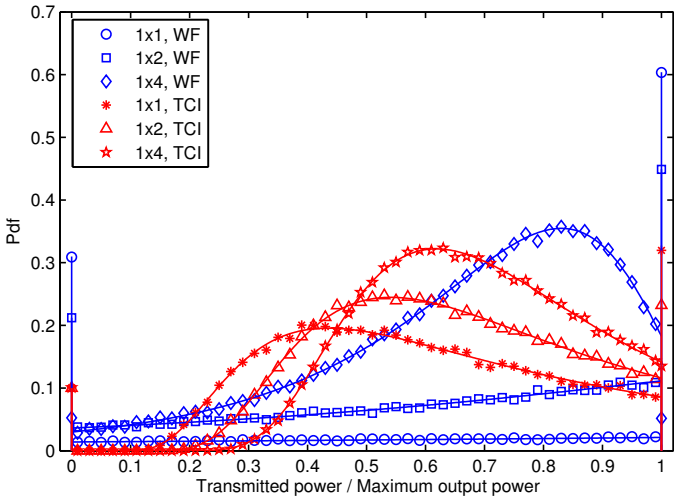

Fig. 5. Transmitted power pdf in a single carrier system for power-controlled MRC and $\overline{P}/P_{\max} = 0.65$ in Rician fading.

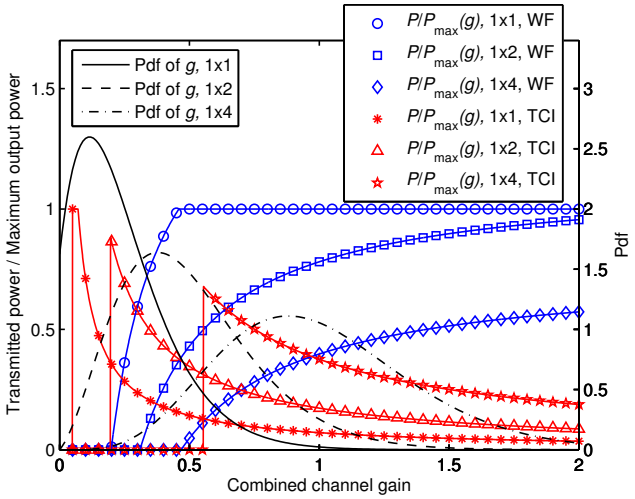

Fig. 6. Pdf of g and $P/P_{\max}$ as a function of g in a single carrier system for power-controlled MRC and $\overline{P}/P_{\max} = 0.35$ in Rician fading.

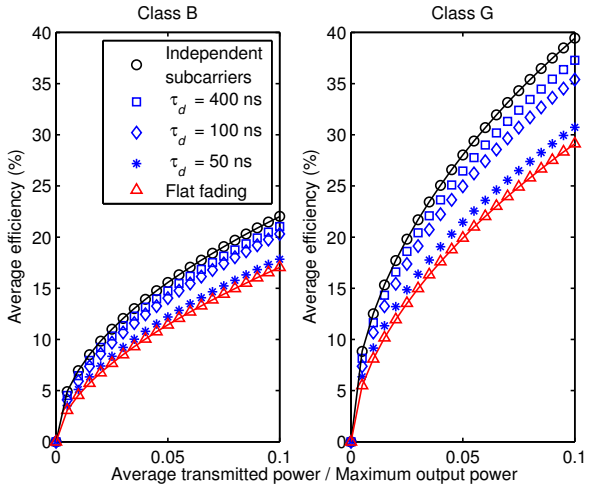

Fig. 7. Average PA efficiency as a function of $\overline{P}/P_{\max}$ in the SISO FCI OFDM system.

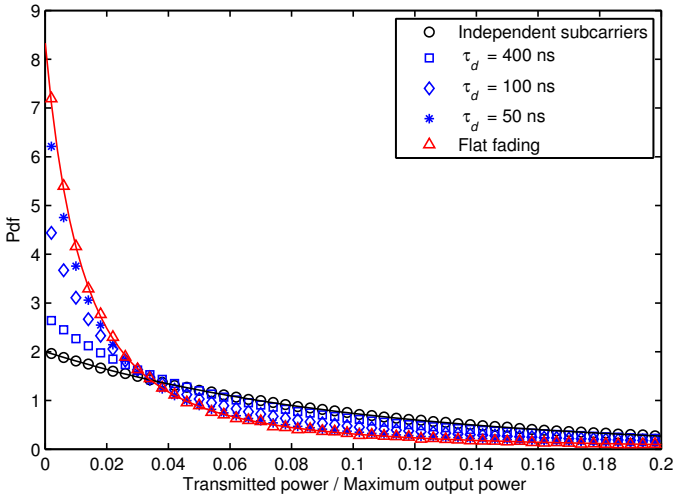

Fig. 8. Transmitted power pdf in the SISO FCI OFDM system when $\overline{P}/P_{\max} = 0.1$.

pdf towards the maximum slightly improving the average PA efficiency of class B PA.

The assessment of the average efficiency of class G PA is complicated by the nonlinear instantaneous efficiency versus output power. A high average PA efficiency is achieved when there is a peak in the transmitted power pdf either close to $P/P_{\max} = 0.5$ or to the maximum output power. The effect of diversity gain for WF with class G PA is mostly similar to the class B PA case. The only difference is at average power level $\overline{P}/P_{\max} = 0.3 \ldots 0.4$ at which the average efficiency with 1×4 MRC is better than with 1×2 MRC. This can be explained by the high peak in the transmitted power pdf of 1×4 WF in Fig. 4 at $P/P_{\max} = 0.45$. For TCI, increased diversity improves the average PA efficiency at low average transmitted powers and vice versa at high average transmitted powers. As can be seen from Fig. 4 for low average transmitted power levels, increased diversity shifts the peak of the pdf closer to $P/P_{\max} = 0.5$ and thus increases the average PA efficiency. At high average transmitted powers the performance is dominated by the impulses at the maximum output power that are visible in Fig. 5.

B. Effect of channel frequency selectivity to the average PA efficiency

The average PA efficiency in the SISO FCI OFDM system is illustrated in Fig. 7 for different levels of channel frequency selectivity. The number of taps in the considered tapped-delay line channel is set to $L = 7$ and the sampling frequency is set to $f_s = 15.36$ MHz corresponding to the 10 MHz LTE system [40]. The average power levels are limited to $\overline{P}/P_{\max} \leq 0.1$ because the typical output power backoff values for OFDM systems are more than 10 dB [41]. It can be clearly seen that the average PA efficiency of FCI improves with the increased channel frequency selectivity. This can be further clarified by investigating the transmitted power pdfs. The transmitted power pdf under the same setting as in Fig. 7 is shown in Fig. 8 for $\overline{P}/P_{\max} = 0.1$. It is easy to see that the pdf approaches the flat fading case when the rms delay spread approaches zero. Similarly, the pdf approaches the highly frequency selective case with independent subcarriers when the rms delay spread increases.

The average PA efficiency of an OFDM system is considerably lower than that of a single carrier system as can be seen from Figs. 3 and 7. The main reason for this is the high PAPR of OFDM systems that forces to use high output power backoff. Another reason causing the low average PA efficiency for the OFDM system is the exponential shape of the transmitted power pdf (see Fig. 8). The majority of the OFDM samples have the power lower than $\overline{P}$ and correspondingly very low PA efficiency.

C. BER as a function of average PA input SNR

Uncoded binary phase shift keying (BPSK) modulation in the single-carrier system with frequency-nonselective Rayleigh fading is used for all the results presented in this section. The bit error probability of BPSK as a function of instantaneous

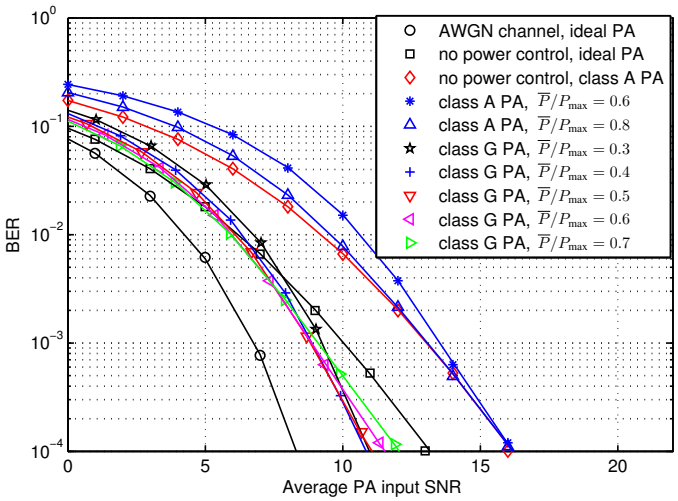

Fig. 9. BER as a function of average PA input SNR in a single carrier system for 1×4 MRC with FCI.

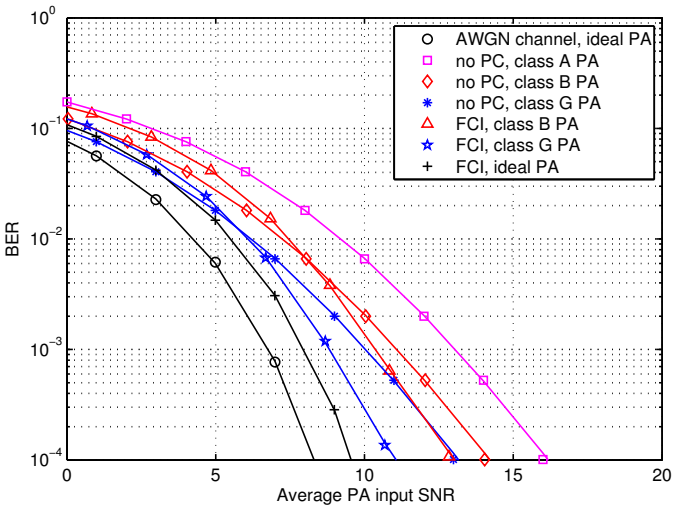

Fig. 10. BER as a function of average PA input SNR in a single carrier system for 1×4 MRC for different PA types.

received SNR is given by $P_b(\gamma) = (1/2)\text{erfc}(\sqrt{\gamma})$, where $\text{erfc}(x)$ is the complementary error function. The results can be extended to other modulations by using their corresponding bit error probability functions. In this section, N_0 is varied for presenting BER as a function of PA input SNR. Each marker in the BER curves corresponds to a single noise level.

In order to have a fair comparison between different algorithms, we first search for the optimal $\overline{P}/P_{\text{max}}$ value for each combination of a power control and diversity method and for the given BER target of 10^{-3}. An example search is illustrated in Fig. 9 where BER as a function of average PA input SNR has been drawn for 1×4 MRC with FCI. For class G PA, the least PA input energy is needed for the target BER when $\overline{P}/P_{\text{max}} = 0.5$. For class A PA, channel inversion is actually harmful and the best performance is achieved without power control. This can be explained by its linear instantaneous efficiency as a function of output power, see (6). The PA input power is constant $P_{\text{sup}} = 2P_{\text{max}}$ for all output powers and thus reduced transmitted power does not bring any energy savings. The results for the ideal PA are also depicted in Fig. 9 for reference. By ideal PA we mean a PA with 100 % efficiency for all output powers. Because of the 100 % efficiency, the average PA input SNR equals the average transmitted SNR for the ideal PA. A similar search for optimal $\overline{P}/P_{\text{max}}$ is done for all cases presented in this section. Figs. 3 and 9 illustrate that different conclusions can be made whether we are interested in transmitter or transceiver efficiency. The average PA efficiency measures only the efficiency of conversion of DC input energy to RF output energy and thus the higher $\overline{P}$ results in better efficiency. However, channel inversion requires low $\overline{P}$ levels in order to be able to invert the deep channel fades. Thus for channel inversion, the optimal average output power is different when maximizing the average PA efficiency or minimizing the input energy per bit.

The effect of the PA type on the BER performance in the 1×4 MRC system is shown in Fig. 10. At the target BER of 10^{-3}, class G PA outperforms class A PA by 3 dB when no power control is used and by 4 dB when FCI is used. The gain from power control is diminished by the nonideal efficiency of a PA. The gain from power control is over 2 dB for ideal PA, less than 1.5 dB for class G, less than 0.5 dB for class B, and no gain at all for class A PA. In Fig. 10, the BER with no power control and ideal PA equals that of class G PA because $\eta(P_{\text{max}}) = 100$ % for class G PA. The effect of nonideal PA to the transceiver energy efficiency illustrated in Fig. 10 would not have been visible if traditional received or transmitted SNR had been used instead of PA input SNR because they do not take into account the efficiency of the PA.

The performance of 2×2 transmission diversity methods is compared in Fig. 11 where BER as a function of average PA input SNR is shown for class B and the ideal PA. Even though mathematical analysis of EGT was not feasible, we have connected the related simulated markers with dashed line for better visibility. When the ideal PA is considered, MRT has the best performance as expected because MRT is the optimal transmitter diversity technique in the sense that it maximizes the received SNR. As the average PA input SNR equals the average transmitted SNR for the ideal PA, the curves for the ideal PA also represent performance comparison with a traditional SNR metric. When class B PA is used, there is a performance loss of 2.2 dB compared to the ideal PA and the performance is the worst among the compared methods. The PAs for MRT have to be dimensioned for the maximum output power at $\overline{P}$. However, the average transmitted power per antenna is $\overline{P}/2$ resulting in losses when a nonideal PA is used. The best performance for class B PA at the target BER of 10^{-3} is achieved when EGT is combined with FCI. This requires the feedback of full channel knowledge, i.e. both phase and gain information. When only phase or gain information is fed back, the best transmission strategies with class B PA are EGT with no power control and AS with FCI, respectively. The performance loss compared to EGT with FCI is approximately 0.5 dB in both cases. If AS with no power control is used, the amount of feedback is limited to one bit and the loss compared to EGT with FCI is 1.5

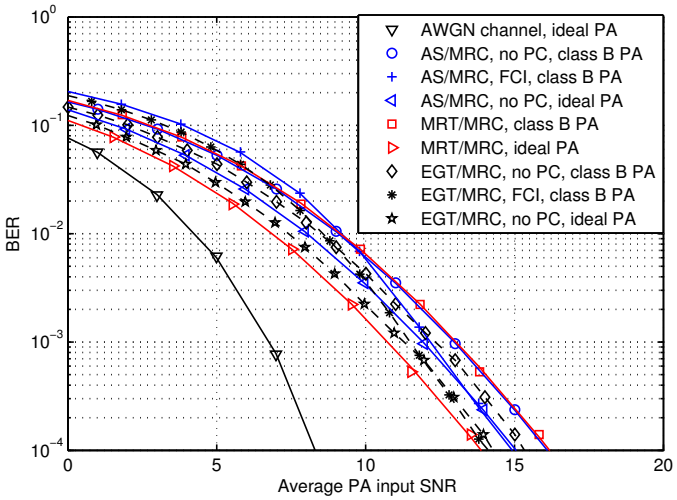

Fig. 11. BER as a function of average PA input SNR in a single carrier system for 2×2 transmission diversity methods.

dB. The results in Fig. 11 illustrate that in transceiver energy efficiency evaluation the average PA input SNR should be used instead of the average transmitted SNR in order to avoid wrong conclusions.

VI. Conclusions

In this paper, we study the transmitter and transceiver energy efficiencies of power-adaptive MIMO diversity systems. We present previously unpublished transmitted power pdfs and use them for analysis of the average PA efficiency and the average PA input power for several PA types. When the transmitted power is not constant, average efficiency should be used for measuring the efficiency of a PA. We show that the increased diversity improves the average efficiency of TCI and decreases the average efficiency of WF. This phenomenon is explained by the shape of transmitted power pdfs. We also demonstrate that larger frequency selectivity of the channel improves the average PA efficiency of an OFDM system with channel inversion. The BER as a function of average PA input SNR is introduced as a new metric that can be used for transceiver energy efficiency evaluation. We compare the BER performance of several diversity methods using the average PA input SNR. We show that the performance improvement from power control diminishes due to the nonideal efficiency of a PA. As an extreme case, we illustrate that channel inversion is harmful when the instantaneous PA efficiency increases linearly with output power. We also demonstrate that even though MRT achieves better received SNR than EGT, it requires more PA input energy per correctly received bit when the PA has nonideal efficiency. These conclusions could not have been made with traditional SNR metrics because they do not take into account the efficiency of the PA. The average transmitted SNR is equivalent to the average PA input SNR only when the PA has ideal 100% efficiency over its whole output power range.

The analytical methodology presented in this paper can be applied to a wide range of transmission methods. For example, it is straightforward to extend the analysis for the quadrature amplitude modulated (QAM) input signal. In the single carrier QAM system, the amplitude of the input signal and transmitter weighting by power control or transmitter diversity are independent. This simplifies the analysis of expected values, such as the average PA efficiency and the average PA input SNR, because of the expected value of a product of random variables equals the product of the expected values of the random variables when the random variables are uncorrelated. When the transmission and reception methods are fixed, the average PA efficiency can be used for comparing different PA designs. On the other hand when the used PA is fixed, BER as a function of PA input SNR can be used to evaluate which transmission method reaches the target BER with the least PA input energy. To enable accurate analysis, we have defined a system almost free from nonlinearities. The PA is modelled as a soft limiter, i.e. it is linear until the maximum output power at which the signal amplitude is saturated. In the studied OFDM system, there are no nonlinear effects when the output power backoff is selected large enough to almost always avoid saturation at the PA output. It remains as further work to include more realistic PA models, such as dynamic voltage controlled PAs, and study the effect of their nonlinearities in the OFDM system. Another potential research direction would be to extend the analysis to consider also MIMO transmission methods with nonconstant bit rate.

Acknowledgment

The authors would like to thank Adrian Kotelba, Jens Elsner, and Friedrich K. Jondral for their help.

References

[1] A. Mämmelä, A. Kotelba, M. Höyhtyä, and D. P. Taylor, "Relationship of average transmitted and received energies in adaptive transmission," *IEEE Trans. Veh. Technol.*, vol. 59, pp. 1257–1268, Mar. 2010.

[2] A. Fehske, G. Fettweis, J. Malmodin, and G. Biczók, "The global footprint of mobile communications: The ecological and economic perspective," *IEEE Commun. Mag.*, vol. 49, pp. 55–62, Aug. 2011.

[3] L. M. Correia *et al.*, "Challenges and enabling technologies for energy aware mobile radio networks," *IEEE Commun. Mag.*, vol. 48, pp. 66–72, Nov. 2010.

[4] A. J. Goldsmith and P. P. Varaiya, "Capacity of fading channels with channel side information," *IEEE Trans. Inf. Theory*, vol. 43, no. 6, pp. 1986–1992, November 1997.

[5] F. H. Raab *et al.*, "Power amplifiers and transmitters for RF and microwave," *IEEE Trans. Microw. Theory Tech.*, vol. 50, pp. 814–826, Mar. 2002.

[6] Y. Neuvo, "Cellular phones as embedded systems," in *Proc. IEEE ISSCC*, San Francisco, CA, Feb. 2004, pp. 32–37.

[7] F. H. Raab, "Average efficiency of class-G power amplifiers," *IEEE Trans. Consum. Electron.*, vol. 32, no. 2, pp. 145–150, January-February 1986.

[8] J. F. Sevic, "Statistical characterization of RF power amplifier efficiency for CDMA wireless communication systems," in *Proc. Wireless Communications Conference*, Boulder, CO, Aug. 1997, pp. 110–113.

[9] B. Sahu and G. A. Rincón-Mora, "A high-efficiency linear RF power amplifier with a power-tracking dynamically adaptive buck-boost supply," *IEEE Trans. Microw. Theory Tech.*, vol. 52, pp. 112–120, Jan. 2004.

[10] J. Deng, P. S. Gudem, L. E. Larson, and P. M. Asbeck, "A high average-efficiency SiGe HBT power amplifier for WCDMA handset applications," *IEEE Trans. Microw. Theory Tech.*, vol. 53, pp. 529–537, Feb. 2005.

[11] S. Boumard and A. Mämmelä, "The effect of power control on the average power amplifier efficiency," in *Proc. IEEE PIMRC*, Istanbul, Turkey, Sep. 2010, pp. 629–633.

[12] K. Han, Y. Choi, S. Choi, and Y. Kwon, "Power amplifier characteristic-aware energy-efficient transmission strategy," in *Proc. 6th International IFIP-TC6 Networking Conference*, Atlanta, GA, May 2007, pp. 37–48.

[13] A. He *et al.*, "Power consumption minimization for MIMO systems – A cognitive radio approach," *IEEE J. Sel. Areas Commun.*, vol. 29, pp. 469–479, Feb. 2011.

[14] Y. Chen, S. Zhang, and S. Xu, "Impact of non-ideal efficiency on bits per joule performance of base station transmissions," in *Proc. IEEE VTC Spring*, Budapest, Hungary, May 2011.

[15] K. S. Shanmugan, *Digital and Analog Communication Systems*. John Wiley & Sons, 1979, ch. 8.6.2.

[16] O. Apilo, M. Lasanen, A. Mämmelä, and F. K. Jondral, "Average efficiency of power amplifiers in power-controlled systems with multi-antenna diversity," in *Proc. WTS*, New York, Apr. 2011.

[17] N. L. Johnson, S. Kotz, and N. Balakrishnan, *Continuous Univariate Distributions, Volume 2*, 2nd ed. New York, NY: John Wiley & Sons, Inc., 1995.

[18] B. Glance and L. J. Greenstein, "Frequency-selective fading effects in digital mobile radio with diversity combining," *IEEE Trans. Commun.*, vol. 31, pp. 1085–1094, Sep. 1983.

[19] S. C. Cripps, *RF Power Amplifiers for Wireless Communications*. Norwood, MA: Artech House, 1999.

[20] P. Reyneart and M. Steyaert, *RF Power Amplifiers for Mobile Communications*. Dordrecht, The Netherlands: Springer, 2006.

[21] J. S. Walling, S. S. Taylor, and D. J. Allstot, "A class-G supply modulator and class-E PA in 130 nm CMOS," *IEEE J. Solid-State Circuits*, vol. 44, no. 9, pp. 2339–2347, September 2009.

[22] R. Darraji, F. M. Ghannouchi, and O. Hammi, "A dual-input digitally driven Doherty amplifier architecture for performance enhancement of Doherty transmitters," *IEEE Trans. Microw. Theory Tech.*, vol. 59, no. 5, pp. 1284–1293, May 2011.

[23] H. Ochiai and H. Imai, "On the distribution of the peak-to-average power ratio in OFDM signals," *IEEE Trans. Commun.*, vol. 49, pp. 282–289, Feb. 2001.

[24] J. N. Laneman, D. N. C. Tse, and G. W. Wornell, "Cooperative diversity in wireless networks: Efficient protocols and outage behavior," *IEEE Trans. Inf. Theory*, vol. 50, pp. 3062–3080, Dec. 2004.

[25] D. G. Brennan, "Linear diversity combining techniques," *Proceedings of the IRE*, vol. 47, pp. 1075–1102, Jun. 1959.

[26] S. Thoen, L. V. der Perre, B. Gyselinckx, and M. Engels, "Performance analysis of combined transmit-SC/receive-MRC," *IEEE Trans. Commun.*, vol. 49, pp. 5–8, Jan. 2001.

[27] T. K. Y. Lo, "Maximum ratio transmission," *IEEE Trans. Commun.*, vol. 47, pp. 1458–1461, Oct. 1999.

[28] G. Ganesan and P. Stoica, "Utilizing space-time diversity for wireless communications," *Wireless Personal Communications*, vol. 18, pp. 165–178, Aug. 2001.

[29] M. Kang and M.-S. Alouini, "Largest eigenvalue of complex Wishart matrices and performance analysis of MIMO MRC systems," *IEEE J. Sel. Areas Commun.*, vol. 21, pp. 418–426, Apr. 2003.

[30] K. C. Hwang and K. B. Lee, "Efficient weight vector representation for closed-loop transmit diversity," in *Proc. IEEE ICC*, New York, Apr.-May 2002, pp. 732–736.

[31] D. J. Love and R. W. Heath Jr., "Equal gain transmission in multiple-input multiple-output wireless systems," *IEEE Trans. Commun.*, vol. 51, pp. 1102–1110, Jul. 2003.

[32] S.-H. Tsai, "Equal gain transmission with antenna selection in MIMO communications," *IEEE Trans. Wireless Commun.*, vol. 10, pp. 1470–1479, May 2011.

[33] T. Pe and H. Drygas, "An alternative representation of noncentral beta and F distributions," *Statistical Papers*, vol. 47, pp. 311–318, Mar. 2006.

[34] R. Bartoszýnski and M. Niewiadomska-Bugaj, *Probability and Statistical Inference*, 2nd ed. Hoboken, NJ: John Wiley & Sons, Inc., 2008.

[35] A. Clark, P. J. Smith, and D. P. Taylor, "Instantaneous capacity of OFDM on Rayleigh-fading channels," *IEEE Trans. Inf. Theory*, vol. 53, pp. 355–361, Jan. 2007.

[36] A. Papoulis, *Probability, Random Variables, and Stochastic Processes*, 2nd ed. New York: McGraw-Hill, 1984.

[37] V. K. Rohatgi, *An Introduction to Probability Theory Mathematical Statistics*. New York: Wiley, 1976.

[38] F. W. J. Olver, D. W. Lozier, R. F. Boisvert, and C. W. Clark, Eds., *NIST Handbook of Mathematical Functions*. New York: Cambridge University Press, 2010.

[39] J. G. Proakis, *Digital Communications*, 5th ed. New York: McGraw-Hill, 2008.

[40] *3GPP TR 25.814, Physical layer aspects for evolved Universal Terrestrial Radio Access (UTRA) (Release 7)*, 3GPP Technical Specification, Rev. 7.1.1, Sep. 2006.

[41] D. Falconer, S. L. Ariyavisitakul, A. Benyamin-Seeyar, and B. Eidson, "Frequency domain equalization for single-carrier broadband wireless systems," *IEEE Commun. Mag.*, vol. 40, pp. 58–66, Apr. 2002.

Olli Apilo (S'11) was born in Joensuu, Finland, in 1980. He received the M.Sc. (Tech.) degree in communications engineering from the Helsinki University of Technology, Espoo, Finland, in 2006. He is currently pursuing the Ph.D. degree in communications engineering at the University of Oulu, Finland.

From 2004 to 2006, he was a Research Trainee with the Networking Laboratory, Helsinki University of Technology. Since 2006, he has been a Research Scientist with VTT Technical Research Centre of Finland, Oulu. From 2010 to 2011, he was a Visiting Research Scientist with the Communications Engineering Laboratory, Karlsruhe Institute of Technology, Germany. His research interests include the techniques improving the spectral and energy efficiency of wireless communications and their analysis.

Mika Lasanen was born in Uusikaupunki, Finland, in 1972. He received the M.Sc. (Tech.) degree in electrical engineering (with honors) from the University of Oulu in 1998. From 1998 to 2012 he worked as a Research Scientist and Project Manager in various research projects and customer assignments at VTT Technical Research Centre of Finland. Since 2012, he has been a Team Leader of VTT's Wireless Access research team. His current research topics are related to improving energy efficiency of wireless communications.

Sandrine Boumard (M'98) received her M.S. degree in Electronics and Communication Systems from the "Institut National des Sciences Appliquées", INSA, in Rennes, France, in 1998. She also received the Master of Advanced Studies (DEA) in Electronics, Systems, Radar and Radiocommunications in 1998. She has since been working at VTT as a Research Scientist. Her interests are in physical layer algorithms, especially in synchronization, estimation, signal processing, mainly but not only for OFDM systems and more generally for wireless communications.

Aarne Mämmelä (M'83-SM'99) was born in Vihanti, Finland, in 1957. He received the M.Sc. (Tech.), Lic.Sc. (Tech.), and D.Sc. (Tech.) degrees (all with honors) from the University of Oulu, Oulu, Finland, in 1983, 1988, and 1996, respectively, all in electrical engineering. His main field of study was telecommunications.

From 1982 to 1993, he was an Assistant, Research Scientist, acting Associate Professor, and acting Professor with the Telecommunication Laboratory, University of Oulu, where he carried out research on adaptive algorithms in spread-spectrum systems. From 1990 to 1991, he was a Visiting Research Scientist with the University of Kaiserslautern, Kaiserslautern, Germany. In 1993, he joined VTT Technical Research Centre of Finland, Oulu, as a Senior Research Scientist. He has been a Research Professor of digital signal processing in wireless communications since 1996. From 1996 to 1997, he was a Postdoctoral Research Scientist with the University of Canterbury, Christchurch, New Zealand. He has been a Docent that corresponds to an Adjunct Professor with the University of Oulu since 2004. In 2001-2011, he regularly organized a course and gave one third of the lectures on research methodology for doctoral students in engineering at the University of Oulu. His research interests are in adaptive, cognitive, and nonlinear systems and in energy efficiency in telecommunications.